

# Evaluation and Analysis Methods of Motor Characteristics in JFE Steel†

TODA Hiroaki\*<sup>1</sup> ODA Yoshihiko\*<sup>2</sup> ZAIZEN Yoshiaki\*<sup>3</sup>

## Abstract:

*The influence of material hardness and thickness of non-oriented electrical steel sheets on iron loss deterioration due to punching and shearing process was investigated. The ratio of iron loss deterioration shows a strong correlation with hardness and thickness of the material, and the deterioration ratio is smaller as the increase of material hardness and the decrease of material thickness. The harder and thinner material has a shorter droop height in the sheared edge, and the ratio of iron loss deterioration has a good correlation with the droop height in the sheared edge. The measured iron loss of a model interior permanent magnet synchronous motor (IPMSM) agreed well with the calculated motor iron loss by considering the deterioration of magnetic properties due to punching process. The magnetic properties of non-oriented electrical steel sheets under compressive stress were also investigated. The deterioration ratio of iron loss under compressive stress decreases with the decrease of material magnetostriction, and 6.5% Si steel sheet of nearly zero magnetostriction showed an extremely low deterioration of iron loss. In the tested IPMSM using 6.5% Si steel, the motor iron loss showed a little change after the heat shrinking.*

## 1. Introduction

Non-oriented electrical steel sheets are widely used as core materials for motors, generators, and other equipment, and are critical soft magnetic materials which support today's society. In recent years, requirements for higher performance and energy saving in all

types of motors have become increasingly strict from the viewpoint of efficient utilization of energy, and higher performance responding to these requirements is demanded in non-oriented electrical steel sheets<sup>1-3</sup>). On the other hand, in order to achieve higher performance and higher efficiency in motors, selection of core materials corresponding to their particular features and use of the optimum materials are also considered necessary<sup>4-6</sup>).

Motor cores are generally manufactured by punching of non-oriented electrical steel sheets, but in that process, it is known that the magnetic properties of the electrical steel sheet are deteriorated by the plastic strain and elastic strain generated around the punching edge<sup>7-11</sup>). Although analyses of motor characteristics considering strain during punching have been performed recently<sup>12</sup>), the relationship between iron loss and the amount of strain is based on the results of actual measurements of iron loss.

The magnetic properties of non-oriented electrical steel sheets are normally measured and evaluated by sheared Epstein samples with the width of 30 mm and length of 280 mm in accordance with JIS C 2552 (JIS: Japanese Industrial Standards). In many cases, however, the tooth width and yoke width of stator on actual motors are narrower than 30 mm. Thus, clarification of the effect of material characteristics on iron loss deterioration during punching is extremely important, but there are few examples of reports on this subject<sup>7,8</sup>).

In order to reduce iron loss, use of materials in which resistivity is increased by high Si addition, etc. to the base material or use of thin-gauge materials has continued to increase in recent years<sup>13</sup>). Therefore, JFE Steel

† Originally published in *JFE GIHO* No. 36 (Aug. 2015), p. 24-31



\*<sup>1</sup>Dr. Eng.,  
Staff Deputy General Manager,  
Electrical Steel Business Planning Dept.,  
JFE Steel



\*<sup>2</sup>Senior Researcher Deputy General Manager,  
Electrical Steel Res. Dept.,  
Steel Res. Lab.,  
JFE Steel



\*<sup>3</sup>Senior Researcher Deputy Manager,  
Electrical Steel Res. Dept.,  
Steel Res. Lab.,  
JFE Steel

studied the effects of hardness and sheet thickness on iron loss deterioration in non-oriented electrical steel sheets by performing shearing process simulating the punching process. The results of that study are reported in the following Chapter 2<sup>14</sup>).

Motor iron loss measurements were also performed by trial-fabrication of interior permanent magnet synchronous motors (IPMSM). Motor iron loss was calculated by using the magnetic properties obtained from specimens prepared by shearing the sample material to approximately the same width (10, 5 mm) as the tooth width and yoke width of the trial-fabricated stator and the magnetic properties of the Epstein sample, and then the effect of changes in magnetic properties due to processing on those calculated values was evaluated. The results are reported in Chapter 3<sup>15,16</sup>).

Although the magnetic properties of electrical steel sheets are generally measured under a non-stress condition, because heat shrinking is performed in order to fix the core in air conditioner compressor motors and other devices, these electrical steel sheets are used under a condition in which compressive strain of 10–100 MPa is applied to the sheet<sup>17</sup>). In addition, heat shrinking or pressing into a frame is frequently performed in order to fix the core in cases where segmented cores are used to increase steel sheet yield during punching. Since it is known that magnetic properties are greatly deteriorated when compressive stress is applied to electrical steel sheets in this manner, the magnetic properties of various types of electrical steel sheets have been evaluated under compressive stress<sup>18–20</sup>). Nevertheless, there have been few reports on the effects of material characteristics on iron loss under compressive stress<sup>21</sup>).

In particular, Si reduces magnetic anisotropy and since iron loss is effectively reduced by an increase in resistivity, Si is an element with a long history of use, and then approximately 2–3% Si is added to high grade electrical steel sheets. Therefore, the compressive stress characteristics of electrical steel sheets in which the Si content was changed to various levels were examined. The results were studied from the viewpoint of magnetostriction, and properties before and after heat shrinking were evaluated by actually trial-fabricating IPMSM. These results are reported in Chapter 4<sup>22,23</sup>).

## 2. Influence of Hardness and Sheet Thickness of Non-Oriented Electrical Steel Sheets on Iron Loss Deterioration during Shearing Process

### 2.1 Experimental Method

Although processing of motor cores is generally performed by punching, in this study, specimens were pre-

pared by shearing process which simulated punching.

As materials for evaluation of the influence of hardness, materials with the sheet thickness of 0.35 mm and crystal grain size of 70  $\mu\text{m}$  were prepared from base materials with different Si contents, and to evaluate the influence of sheet thickness, materials with thicknesses of 0.20 to 0.50 mm and the grain size of 70  $\mu\text{m}$  (hardness HV0.5: 200 in all cases) were prepared from a base material with the same Si content of 3 mass%.

Specimens with widths of 30 mm and 5 mm were prepared from the rolling direction (L-direction) and the perpendicular to the rolling direction (C-direction) of these materials by shearing process with the clearance of 15  $\mu\text{m}$ . After joining the 5 mm width specimens together with cellophane tape to form a specimen with the width of 30 mm, magnetic measurements were performed by the Epstein test method, and iron loss ( $W_{15/50}$ ) was evaluated by the average value of the L-direction and C-direction specimens. The deterioration ratio of iron loss  $\Delta W$  (%) due to shearing process was calculated by the following Eq. (1) by using the iron loss of the 30 mm width specimen  $W$  (30 mm) and the iron loss of the 5 mm width specimen  $W$  (5 mm).

$$\Delta W (\%) = [W (5 \text{ mm}) - W (30 \text{ mm})] / W (30 \text{ mm}) \times 100 \quad \dots\dots\dots (1)$$

### 2.2 Experimental Results and Discussion

The influences of material hardness and material thickness on the deterioration ratio of iron loss ( $W_{15/50}$ ) are shown in **Figs. 1** and **2**, respectively. The deterioration ratio of iron loss shows good correlations with both material hardness and material thickness, and it can be understood that the deterioration ratios of iron loss on high hardness materials and thin-gauge materials are small.

In order to investigate the reason for these results, the hardness distribution in the edge part with shearing process was measured with a micro Vickers hardness test. The obtained hardness distribution was evaluated by the hardness increase ratio (%) in comparison with the part which was not affected by shearing.

The results for the materials with the thickness of 0.35 mm and different base material hardnesses (HV0.5: 154, 217) are shown in **Fig. 3**, and the results for materials with the same base material hardness and different material thicknesses (0.20, 0.50 mm) are shown in **Fig. 4**. In the thick-gauge, low hardness material, the area of increased hardness in the vicinity of the sheared edge has become larger. From this, it can be estimated that the amount of plastic deformation due to shearing is large; therefore, the droop height at the sheared edge was measured. **Figure 5** shows an example of the cross-

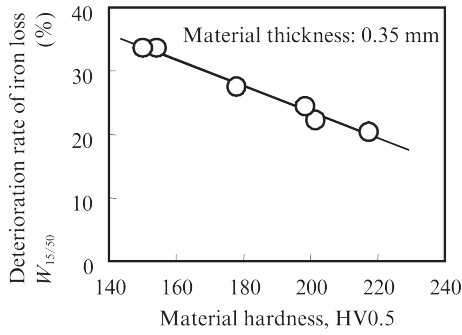


Fig. 1 Influence of material hardness on iron loss deterioration

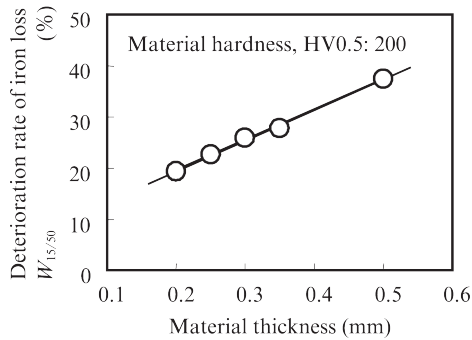
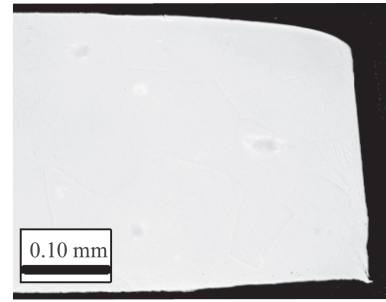
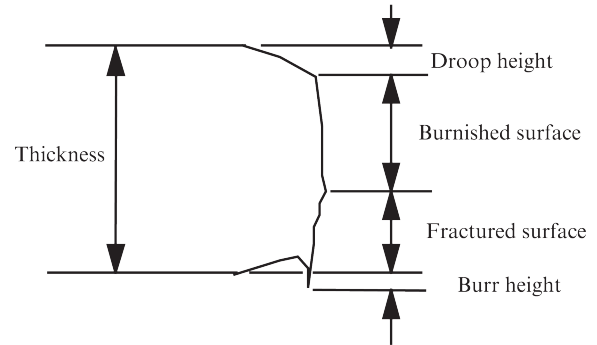


Fig. 2 Influence of material thickness on iron loss deterioration



(a) Optical microscope image of cross section of sheared edge of 0.35 mm thickness material



(b) Schematic view of cross section of sheared edge

Fig. 5 Optical image and schematic view of sheared edge

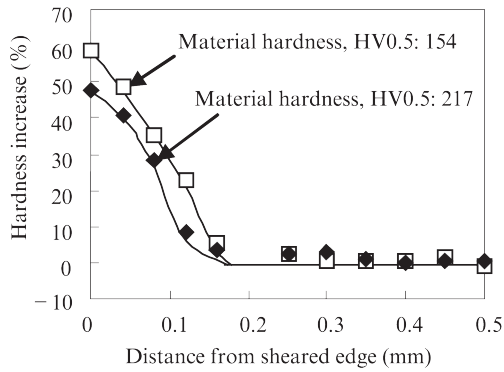


Fig. 3 Influence of material hardness on distribution of hardness increase near sheared edge of 0.35 mm thickness material

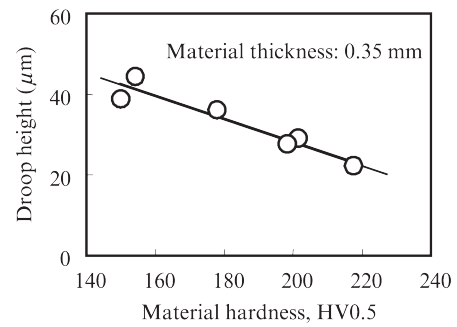


Fig. 6 Influence of material hardness on droop height

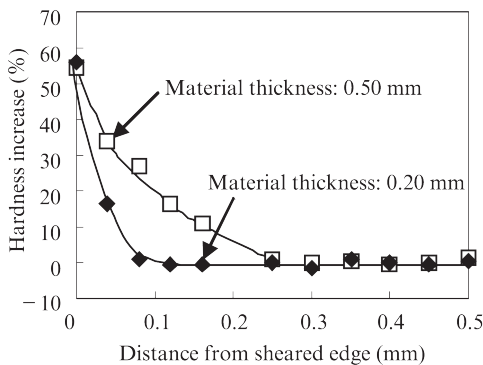


Fig. 4 Influence of material thickness on distribution of hardness increase near sheared edge for the same hardness (HV0.5: 200) material

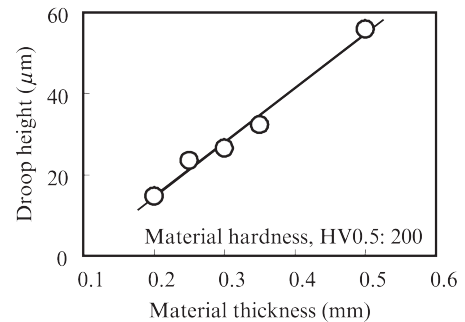


Fig. 7 Influence of material thickness on droop height

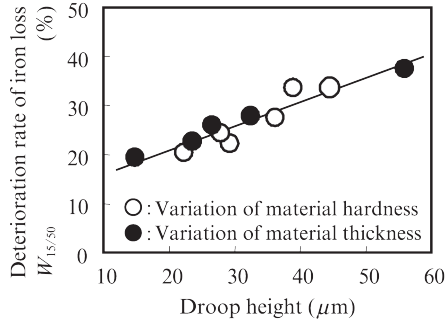


Fig. 8 Influence of droop height on iron loss deterioration

section observation of the sheared edge (0.35 mm thickness material) and a schematic diagram of the sheared edge. **Figures 6 and 7** show the influence of material hardness and material thickness on droop height, respectively; it can be understood that the droop height is large in materials with low hardness and large thickness.

Since the droop height was considered to reflect the deterioration ratio of iron loss, the relationship between the droop height and deterioration ratio of iron loss  $\Delta W$  (%) was investigated. The results are shown in **Fig. 8**.

From these results, iron loss deterioration and droop height display a good correlation, independent of variations of the hardness or thickness of the base material. Therefore, it is considered that the magnitude of strain given during shearing process can be evaluated from the droop height, and the deterioration ratio of iron loss decreases by use of higher hardness and/or thinner gauge base material because the amount of strain introduced in the vicinity of the sheared edge decreases under those conditions. The hardness increase region at the edge with shearing process is approximately one-half of the sheet thickness, and it is thought that plastic strain accumulates within this range. However, it has been reported that the change in the magnetic domain structure due to punching/shearing process occurs up to approximately 2 times the sheet thickness, and there is a region where elastic strain, which influences magnetic properties, is also given to the part of the sheet inward from the region where plastic strain accumulates<sup>9,11</sup>. This notwithstanding, the fact that the influence of plastic strain on iron loss deterioration is large, and the fact that the magnitude of plastic strain due to processing is reflected in the magnitude of elastic strain are conceivable as reasons for the correlation between the droop height at the sheared edge and the deterioration ratio of iron loss. As future work, study including measurement of strain distribution, and analytical calculations of stress, etc. is considered necessary in order to clarify these points.

### 3. Influence of Change in Magnetic Properties by Punching on Calculated Iron Loss in IPMSM

#### 3.1 Experimental Method

The specifications of the IPMSM used in this study are shown in **Table 1**. The rotor has 12 poles, the stator has 18 slots, and the type of winding is concentrated winding. **Table 2** shows the magnetic properties of the Epstein samples of the materials used in the stator core (Average of rolling direction and perpendicular to the rolling direction). Five grades of non-oriented electrical steel sheets with approximately the same hardness and different material thicknesses were used as test materials. In order to clarify the influence of the stator core material, the same rotor was used through all the measurements.

The stator used here was a segmented core type which was prepared by punching the electrical steel sheets so that the rolling direction (L-direction) of the base material coincided with the tooth radial direction, as illustrated in **Fig. 9**. The circumferential direction of the yoke part corresponds approximately to the perpendicular to the rolling direction (C-direction) of the base material. The tooth width and the yoke width are 10 mm and 5.4 mm, respectively. Therefore, 5 and 10 mm width test pieces were prepared by shearing process simulating punching from the 30 mm width Epstein sample. The magnetic property measurements were performed by the same method as that described in the previous chapter.

Table 1 Specifications of tested model interior permanent magnet synchronous motor (IPMSM)

Item	Specification
Stator outer diameter	156 mm
Stator inner diameter	105.2 mm
Stator teeth width	10 mm
Stator yoke width	5.4 mm
Rotor outer diameter	104.6 mm
Rotor inner diameter	40 mm
Air gap	0.3 mm
Stack length	25 mm
Winding	3 $\phi$ Star-Connection

Table 2 Magnetic properties of tested samples

Symbol	Thickness (mm)	Iron loss, $W_{15/50}$ (W/kg)	Iron loss, $W_{10/400}$ (W/kg)	Magnetic flux density, $B_{50}$ (T)	Hardness, HV0.5	Grain size ( $\mu\text{m}$ )
A	0.20	1.97	11.3	1.69	195	86
B	0.25	1.87	12.7	1.70	194	95
C	0.30	2.06	15.0	1.70	191	88
D	0.35	2.14	17.0	1.71	193	92
E	0.50	2.57	25.3	1.72	193	85

(Tests were conducted by using 30 mm width Epstein samples (L + C) as sheared.)

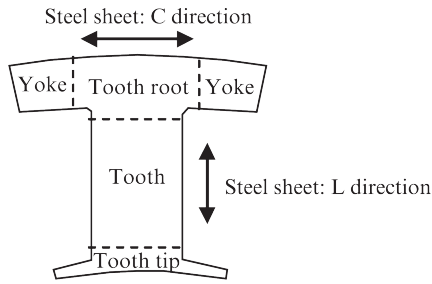


Fig. 9 Schematic structure of segmented stator core

In the measurements of motor characteristics, the characteristics under the conditions of  $2\,500\text{ min}^{-1}$  and  $1\text{ Nm}$  were evaluated after adjusting the temperature of the stator to  $40^\circ\text{C}$ . The drive method was an excited rectangular current with  $120$  electrical degrees per cycle, controlled so that the advance commutation angle of the current phase was  $15^\circ$  (electrical angle). Regarding separation of motor loss, copper loss was obtained from the primary winding resistance and electrical current, and motor iron loss was then obtained by subtracting copper loss and mechanical loss (including windage loss) from total loss.

### 3.2 Experimental and Calculated Results and Discussion

The iron loss deterioration of electrical steel sheets due to shearing process simulating punching was evaluated as  $[W_i - W(30\text{ mm})] / W(30\text{ mm}) \times 100$ , when  $W_i$  is iron loss after shearing to the narrow width, assuming the iron loss value  $W(30\text{ mm})$  of a  $30\text{ mm}$  width test piece (Epstein sample) as a standard, as in the above-mentioned Eq. (1). The influence of the material thickness on the deterioration ratio of iron loss when the sheared width was  $5\text{ mm}$  and  $10\text{ mm}$  is shown in Fig. 10. Although iron loss was evaluated by the general index  $W_{15/50}$  and  $W_{10/400}$ , which is an index of high-frequency iron loss, in both cases, it can be understood that the deterioration ratio of iron loss was smaller with the thin-gauge sheet, and that tendency is remarkable when the sheared width is narrow.

Stator iron loss was calculated based on the follow-

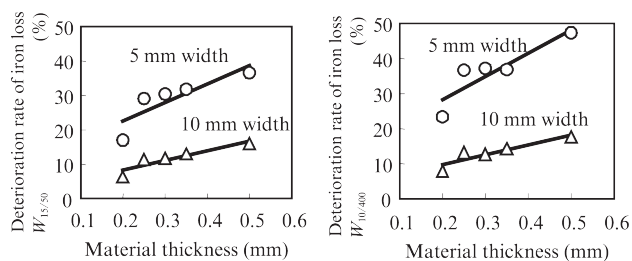


Fig. 10 Influence of material thickness on iron loss deterioration for the sheared width of 5 and 10 mm samples (L + C)

ing equations after obtaining the change of magnetic flux density by an electromagnetic field analysis with using the measured current waveform.

$$P_t = k_h f B_m^\alpha K(B_m) + (\sigma/12) (d^2 f \delta) \int_{1/f} (dB/dt)^2 dt + k_e f \int_{1/f} |dB/dt|^{1.5} dt \dots \dots \dots (2)$$

$$K(B_m) = 1 + (0.65/B_m) \Sigma \Delta B_i \dots \dots \dots (3)$$

where,  $\Delta B_i$  is the variation of flux density during the excursion around a minor loop,  $B_m$  is the maximum value of flux density and  $f$  is frequency. The symbols  $\sigma$ ,  $\delta$ , and  $d$  represent the electrical conductivity, mass and thickness of the steel sheet (iron core), respectively.  $k_h$  and  $\alpha$  are hysteresis loss coefficients and  $k_e$  is an excess eddy current loss coefficient. Iron loss due to the rotating magnetic field was obtained by calculating the iron loss separately for the circumferential direction and the radial direction of the motor, and then adding the two results together.

The above-mentioned loss constants and magnetization curve ( $B$ - $H$  curve) was obtained for the  $30\text{ mm}$  width Epstein sample and test material pieces having approximately the same widths ( $10, 5\text{ mm}$ ) as the stator shape width. The respective results were used, as shown in Table 3. As one example, in the case of material C, the influence of the difference in sheared width on the magnetization curve is shown in Fig. 11. When the sheared width is reduced, the decrease of flux density from the low field through the middle field is remarkable. Accordingly, in order to investigate not only the effect of iron loss, but also the effect of the magnetization curve, calculations were performed under the

Table 3 Material data applied in iron loss calculation

Condition	Data of Magnetization curve	Data of loss constants
X	30 mm Width sample	30 mm Width sample
Y	30 mm Width sample	5 and 10 mm Width samples
Z	5 and 10 mm Width samples	5 and 10 mm Width samples

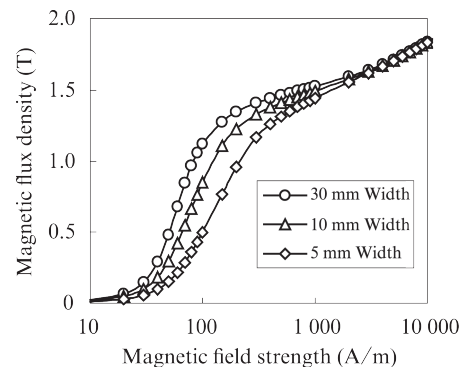


Fig. 11 Influence of sheared width on magnetization curve of material C (L + C)

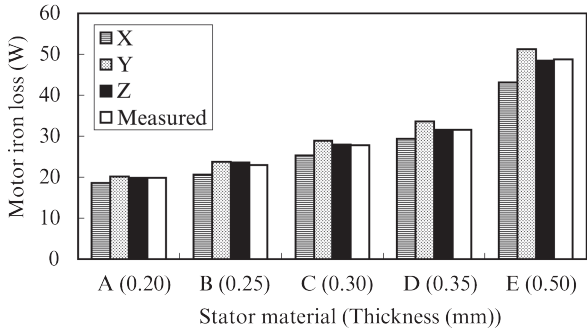


Fig. 12 Comparison of calculated and measured motor iron loss

above-mentioned conditions.

In addition, considering the motor shape and the punching direction of the electrical steel sheets, in all cases, the calculations were performed by inputting the magnetic properties of the L-direction in the tooth part, the magnetic properties of the C-direction in the yoke part and the average magnetic properties of L + C in the tooth tip part and tooth root part.

It has been reported that the rotor iron loss of IPMSM comprises < 10% of motor iron loss, as rotor iron loss is nearly all eddy current loss and hysteresis loss can be ignored<sup>24</sup>). Therefore, only the eddy current loss in Eq. (2) (2nd and 3rd terms on the right side of equation) was calculated, and this was regarded as rotor loss.

A comparison of the calculated and measured values of motor iron loss is shown in Fig. 12. It can be understood that the calculated value of condition X is smaller than the measured value, the calculated value of condition Y is larger than the measured value, and the calculated value of condition Z is approximately the same as the measured value.

The tendency to be too small or too large is remarkable with the thicker materials. The reason for this is considered to be the large change of magnetic properties by shearing.

From this, it can be understood that using the magnetization curve and iron loss value of a test piece width conforming to the actual motor shape is important for improving the accuracy of motor iron loss calculations. Because the difference between the magnetic properties of the Epstein sample and the properties when the sheet is punched to a narrower width than the Epstein sample increases as the thickness of the electrical steel sheet increases, the difference between true motor iron loss and calculated motor iron loss will also increase if the magnetic properties of the Epstein sample are used in calculations.

## 4. Influence of Si Content on Iron Loss under Compressive Stress

### 4.1 Experimental Method

Steels with Si contents of 0.4 to 5.5 mass% were vacuum melted and cast into ingots in the laboratory. The ingots were heated at 1 100°C for 30 min, and hot-rolled steel sheets with the thickness of 2.0 mm were obtained by hot rolling. The hot-rolled steel sheets were then annealed at 900°C×30 s, followed by cold rolling to the thickness of 0.20 mm and finish annealing at 1 000°C×10 s in a 20% H<sub>2</sub>-80% N<sub>2</sub> atmosphere. In order to obtain a material with zero magnetostriction, 6.5% Si steel was produced by preparing a cold-rolled steel sheet of 3.5% Si steel having the sheet thickness of 0.10 mm, performing chemical vapor deposition (CVD) siliconizing at 1 200°C in SiCl<sub>4</sub> gas in the laboratory, and then performing diffusion annealing. Single sheet specimens with the width of 30 mm and length of 180 mm were cut from these sample materials so that the rolling direction was the longitudinal direction of the specimen. In measurements of magnetic properties, a vertical-type double yoke single-sheet tester was used, and iron loss was measured by the wattmeter method. Compressive stress was applied in the specimen longitudinal direction, and the iron loss in the same direction was measured. During these tests, compressive stress of 0.03 MPa was also applied in the sheet thickness direction to prevent buckling of the specimens under compression. In this chapter, compressive stress means the stress applied in the direction of magnetization. As magnetostriction, the peak-to-peak value in case of excitation up to 1.0 T at 400 Hz in the rolling direction was measured by a laser Doppler magnetostriction measurement device.

### 4.2 Experimental Results and Discussion

Figure 13 shows the stress dependency of iron loss of materials with greatly different Si contents ranging from 0.4% to 6.5%. Here, compressive stress is shown

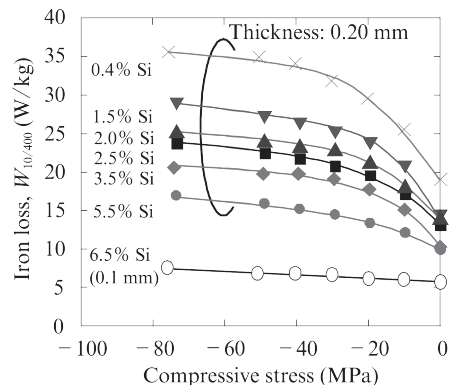


Fig. 13 Effect of compressive stress on iron loss

by the minus (−) sign. From these results, it can be understood that iron loss increases as a result of compressive stress in all the materials, but the increment of iron loss is extremely small in the 6.5% Si steel. However, because the material thickness of the 6.5% Si steel is 0.1 mm, which is different from the thicknesses of the other materials, an evaluation was performed by the deterioration ratio of iron loss defined by the following Eq. (4).

$$\text{(Deterioration ratio of iron loss)} = \frac{\text{(Iron loss under compressive stress of 50 MPa)}}{\text{(Iron loss under no stress)}} \dots\dots (4)$$

**Figure 14** shows the Si dependency of the deterioration ratio of iron loss at the magnetic flux density of 1.0 T and frequency of 400 Hz. It can be understood that the deterioration ratio of iron loss due to applied compressive stress is roughly constant in the range of Si contents of 0.4–3.5%, and the deterioration ratio decreases at higher Si contents than that range.

The physical quantities that change as a result of increased Si contents include resistivity, magnetocrystalline anisotropy, magnetostriction and others. Among these, magnetostriction is a property which changes rap-

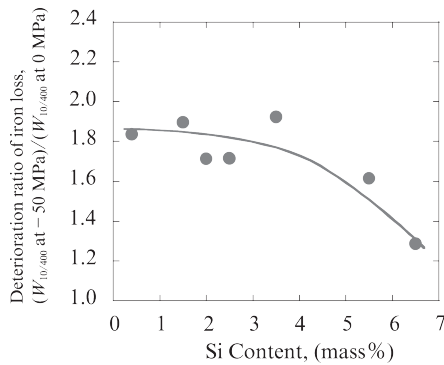


Fig. 14 Effect of Si content on deterioration ratio of iron loss

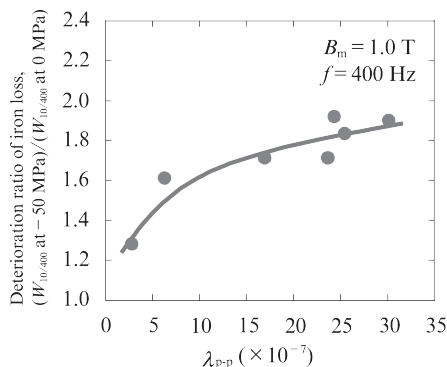


Fig. 15 Effect of magnetostriction on deterioration ratio of iron loss

idly at Si contents over 3.5%, suggesting that the Si dependency of the deterioration ratio of iron loss in Fig. 14 may correspond to a change of magnetostriction. Therefore, the magnetostriction of the various materials was measured, and the relationship between magnetostriction and iron loss deterioration under compressive stress was investigated.

**Figure 15** shows the results when the deterioration ratio of iron loss was arranged by magnetostriction. From these results, it can be understood that there is a good correlation between magnetostriction  $\lambda_{p-p}$  and the deterioration ratio of iron loss, and it is possible to suppress iron loss deterioration due to applied compressive stress by decreasing magnetostriction.

### 4.3 Results of Motor Evaluation by Low Magnetostrictive Material

In the study in Section 4.2, it became clear that decreasing the magnetostriction of the material is effective for suppressing iron loss deterioration under compressive stress. As described above, magnetostriction is extremely small in 6.5% Si steel, and the iron loss deterioration due to application of compressive stress is also small. Therefore, if 6.5% Si steel is used in motors to which compressive stress is applied, for example, motors manufactured by using a heat shrinking, it is considered that the material can demonstrate its intrinsic magnetic properties without deterioration due to heat shrinking.

Therefore, in order to confirm the effect of low magnetostrictive material on motor characteristics, IPMSM with the rated output of 0.3 kW were fabricated by processing by wire-cutting cores having 8 poles, 12 slots and a stacked thickness of 25 mm (**Fig. 16**), using 6.5% Si steel (Thickness: 0.1 mm) and, as a comparison material, 3% Si steel (Thickness: 0.2 mm).

No-load torque for the case where the motor was rotated at  $5\,000\text{ min}^{-1}$  by external drive was measured with a torque meter, and motor loss was obtained from the no-load torque. The no-load iron loss before heat

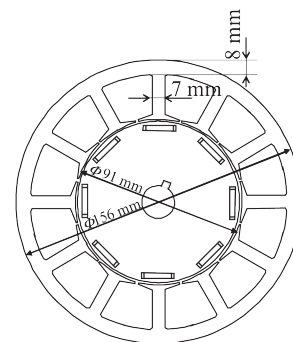


Fig. 16 Schematic diagram of tested interior permanent magnet synchronous motor (IPMSM)

Table 4 Comparison of motor iron loss of tested materials

Material	Thickness (mm)	Heat-shrinking	Motor iron loss (W)
3.0% Si	0.2	Before	21.78
		After	27.41
6.5% Si	0.1	Before	10.27
		After	10.53

shrinking was obtained by subtracting mechanical loss. Next, heat shrinking of the stator in an aluminum alloy case was performed with the heat shrinking allowance of 30  $\mu\text{m}$ , and the no-load iron loss after heat shrinking was measured.

The results of measurements of no-load iron loss before and after heat shrinking are shown in **Table 4**. With the 3% Si steel, which has large magnetostriction, motor iron loss increased by approximately 20% as a result of heat shrinking. On the other hand, with the 6.5% Si steel, which has nearly zero magnetostriction, extremely low iron loss deterioration due to heat shrinking could be detected.

Based on the above-mentioned results, it became clear that reducing the magnetostriction of electrical steel sheets is effective for suppressing iron loss deterioration under compressive stress. In particular, because extremely low deterioration of iron loss due to application of compressive stress can be detected with 6.5% Si steel, which has nearly zero magnetostriction, it can be said that this is the optimum material for motors which are subjected to compressive stress as a result of heat shrinking, etc. with the electrical steel sheets within the range of these experiments.

## 5. Conclusion

In order to achieve high accuracy in motor design, it is necessary to grasp the deterioration of the magnetic properties of the iron core during processing and assembly work in the motor manufacturing process. It is also necessary to reduce the amount of deterioration in those processes, in order to improve motor efficiency. Based on these viewpoints, the following were clarified in this paper.

- (1) To suppress iron loss deterioration during shearing/punching processing, application of high hardness and thin-gauge non-oriented electrical steel sheets, in other words, high grade electrical steel sheets, is effective.
- (2) In cases where electrical steel sheets are to be used as iron core materials in the as-punched condition, application of an iron loss value and a magnetization curve which reflect the actual motor shape is necessary in order to improve the accuracy of motor iron loss calculations using magnetic field analysis.

- (3) The deterioration ratio of iron loss under compressive stress displays a correlation with magnetostriction, which means it is possible to suppress deterioration of iron loss by decreasing the magnetostriction of the electrical steel material. In the case of 6.5% Si steel, which has nearly zero magnetostriction, this study confirmed that the increment of iron loss due to compressive stress is extremely small, and this is also true in motors manufactured by using a heat shrinking.

## References

- 1) Oda, Y.; Kohno, K.; Toda, H. "Recent Development of Non-oriented Electrical Steel Sheet for Automobile Electric Devices." Proc. 4th International Conference Magnetism and Metallurgy (WMM10). Freiberg, Germany, 2010, p. 299–309.
- 2) Toda, H.; Oda, Y.; Kohno, M.; Ishida, M.; Zaizen, Y. "A New High Flux Density Non-Oriented Electrical Steel Sheet and its Motor Performance." IEEE Trans. Magn. 2012, vol. 48, p. 3060–3063.
- 3) Wajima, K.; Marukawa, Y.; Toda, H.; Ichihara, C.; Kosaka, T. "Recent Technical Trends in Magnetic Materials." Proc. 2014 International Power Electronics Conference (IPEC-Hiroshima 2014). Hiroshima, Japan, p. 1984–1989.
- 4) Honda, A.; Kawano, M.; Ishida, M.; Sato, K.; Komatsubara, M. "Efficiency of Model Induction Motor Using Various Non-Oriented Electrical Steels." J. Mater. Sci. Technol. 2000, vol. 16, p. 238–243.
- 5) Toda, H.; Senda, K.; Ishida, M. "Effect of Material Properties on Motor Iron Loss in PM Brushless DC Motor." IEEE Trans. Magn. 2005, vol. 41, p. 3937–3939.
- 6) Toda, H.; Senda, K.; Morimoto, S.; Hiratani, T. "Influence of Various Non-Oriented Electrical Steels on Motor Efficiency and Iron Loss in Switched Reluctance Motor." IEEE Trans. Magn. 2013, vol. 49, p. 3850–3853.
- 7) Schoppa, A.; Schneider, J.; Wuppermann, D. C. "Influence of the manufacturing process on the magnetic properties of non-oriented electrical steels." J. Magn. Magn. Mater. 2000, vol. 215–216, p. 74–78.
- 8) Rygal, R.; Moses, J. A.; Derebasi, N.; Schneider, J.; Schoppa, A. "Influence of cutting stress on magnetic field and flux density distribution in non-oriented electrical steels." J. Magn. Magn. Mater. 2000, vol. 215–216, p. 687–689.
- 9) Senda, K.; Ishida, M.; Nakasu, Y.; Yagi, M. "Effect of Shearing Process on Iron Loss and Domain Structure of Non-oriented Electrical Steel." IEEE Trans. FM. 2005, vol. 125, p. 241–246. (Japanese)
- 10) Kurosaki, Y.; Mogi, H.; Fujii, H.; Kubota, T.; Shinozaki, M. "Importance of punching and workability in non-oriented electrical steel sheets." J. Magn. Magn. Mater. 2008, vol. 320, p. 2474–2480.
- 11) Kaido, C.; Mogi, H.; Fujikura, M.; Yamasaki, J. "Punching Deterioration Mechanism of Magnetic Properties of Cores." IEEE Trans. FM. 2008, vol. 128, p. 545–550.
- 12) Kashiwara, Y.; Fujimura, H.; Okamura, K.; Imanishi, K.; Yashiki, H. "Estimation Model for Magnetic Properties of Stamped Electrical Steel Sheet." IEEE Trans. FM. 2011, vol. 131, p. 567–574. (Japanese)
- 13) Okubo, T.; Hiratani, T.; Toda, H.; Oda, Y. "Recent Development of High Silicon Electrical Steel Sheet." Proc. 6th International Conference Magnetism and Metallurgy (WMM14). Cardiff, UK, 2014, p. 157–167.
- 14) Zaizen, Y.; Toda, H.; Oda, Y.; Senda, K.; Fukumura, M. "Effect of Hardness and Thickness of Electrical Steel Sheet on Iron Loss Deterioration by Shearing Process." 2013 National Convention Record IEE Japan. 2–148, p. 188–189. (Japanese)
- 15) Toda, H.; Zaizen, Y.; Namikawa, M.; Shiga, N.; Oda, Y.; Morimoto, S. "Iron Loss Deterioration by Shearing Process in Non-

- Oriented Electrical Steel with Different Thickness and Its Influence on Estimation of Motor Iron Loss.” IEEJ J. Ind. Appl. 2014, vol. 3, p. 55–61.
- 16) Toda, H.; Zaizen, Y.; Namikawa, M.; Morimoto, S. “Influence of Variation of Magnetic Properties in Electrical Steel by Shearing on Calculated Iron Loss of IPMSM.” 2014 National Convention Record IEE Japan. 5–020, p. 34–35. (Japanese)
  - 17) Yamamoto, K.; Shimomura, E.; Yamada, K.; Sasaki, T. “Effects of External Stress on Magnetic Properties in Motor Cores.” IEEJ Trans. FM. 1997, vol. 117, p. 311–316. (Japanese)
  - 18) Lobue, M.; Sasso, C.; Basso, V.; Fiorillo, F.; Bertotti, G. “Power losses and magnetization process in Fe-Si non-oriented steels under tensile and compressive stress.” J. Magn. Magn. Mater. 2000, vol. 215–216, p. 124–126.
  - 19) Tani, Y.; Daikoku, A.; Nakano, M.; Arita, H.; Yamaguchi, S.; Tode, Y. “Magnetic Power Loss Characteristics of Non-oriented Electrical Steel Sheets under Stress.” J. Magn. Soc. Jpn. 2006, vol. 30, p. 196–200. (Japanese)
  - 20) Miyagi, D.; Miki, K.; Nakano, M.; Takahashi, N. “Influence of Compressive Stress on Magnetic Properties of Laminated Electrical Steel Sheets.” IEEE Trans. Magn. 2010, vol. 46, p. 318–321.
  - 21) Senda, K.; Fujita, A.; Honda, H.; Kuroki, N.; Yagi, M. “Magnetic Properties and Domain Structure of Non-oriented Electrical Steel under Stress.” IEEJ Trans. FM. 2008, vol. 131, p. 884–890. (Japanese)
  - 22) Oda, Y.; Toda, H.; Shiga, N.; Kasai, S.; Hiratani, T. “Effect of Si Content on Iron Loss of Electrical Steel Sheet under Compressive Stress.” IEEJ Trans. FM. 2014, vol. 134, p. 148–153. (Japanese)
  - 23) Oda, Y.; Toda, H.; Shiga, N.; Kasai, S.; Hiratani, T. “Effect of Si Content on Iron Loss of Electrical Steel Sheet Under Compressive Stress.” IEEE Trans. Magn. 2014, vol. 50, 2002304.
  - 24) Yamazaki, K.; Seto, Y.; Tanida, M. “Iron Loss Analysis of IPM Motor Considering Carrier Harmonics.” IEEJ Trans. IA. 2005, vol. 125, p. 758–766. (Japanese)